

A NEW SOLUTION APPROACH FOR THE NONLINEAR DYNAMIC MODEL OF MOLTEN SALT REACTORS

Hüseyin AYHAN

FİGES Engineering, Nuclear Technology Department, Çankaya, Ankara, Turkey, 06690

huseyin.ayhan@figes.com.tr

ERGİMİŞ TUZ REAKTÖRLERİNİN DOĞRUSAL OLMAYAN DİNAMİK MODELİ İÇİN YENİ BİR ÇÖZÜM YAKLAŞIMI

Abstract:

The reactor dynamic modeling of the Molten Salt Reactors is very important due to the circulating liquid fuel in the primary loop. The delayed neutron precursors generated in the core may decay in locations of low importance for criticality and even out of the core. Therefore, determining the amount of the prompt and delayed neutrons, and reactivity feedback are very important for the reactor control. In this study, a new reactor dynamics model is proposed to determine these crucial parameters along with other reactor parameters and transient behavior of the system. The thermal-hydraulic model is adopted differently from the ones available in literature. Point kinetic equations in nonlinear form are linearized and derived in state-space form. A new solution approach for the nonlinear dynamic model of molten salt reactors was achieved in addition to a MATLAB-Simulink model.

Özet:

Erimiş Tuz Reaktörlerinin reaktör dinamik modellemesi, birinci çevrimde dolaşmakta olan sıvı yakıt nedeniyle çok önemlidir. Çekirdekte üretilen gecikmiş nötronlar kritiklik açısından düşük önemdeki bölgelerde ve hatta kor dışında bozulabilir. Bu nedenle, ani ve gecikmiş nötronlar ile reaktivite geri besleme miktarının belirlenmesi reaktör kontrolü açısından oldukça önemlidir. Bu çalışmada, bu kritik parametreler ile diğer reaktör parametrelerini ve sistemin zamana bağlı davranışını belirlemek için yeni bir reaktör dinamiği modeli önerilmiştir. Termal-hidrolik model, literatürde bulunanlardan farklı olarak oluşturulmuştur. Doğrusal olmayan formdaki nokta kinetik denklemler doğrusallaştırılmış ve durum-uzay formunda ifade edilmiştir. Ergimiş tuz reaktörlerinin lineer olmayan dinamik modeli için yeni bir yaklaşım ve MATLAB-Simulink modeli elde edilmiştir

Keywords: Molten Salt Reactor (MSR), Reactor dynamics, Point kinetics, State-space form, Linearization

Anahtar kelimeler: Ergimiş Tuz Reaktörü (ETR), Reaktör dinamiği, Nokta kinetik, Durum-uzay formu, Lineerleştirme

1. Introduction

The Molten Salt Reactor (MSR) is one of the six reactors selected as Generation-IV reactors to be designed. One of the most important distinguishing feature of MSR design is that the fuel circulates through the primary circuit and goes out of the core. Of course, this design has advantages as well as significant challenges. One of the design challenges is related with reactor dynamics. Since the fuel itself circulates through the system and remains outside the

core therefore loss of delayed neutrons outside the core will affect the reactor control mechanism.

In terms of neutron kinetics, the modeling of these reactors is similar to that of solid fuel used in conventional reactors. For the modeling, transit time, during which fuel salt stays outside the core, has to be taken into account. Therefore, a time multiplier term for the delayed neutron precursor is added to neutron kinetics equations (Shimazu, 1978). On the other hand, the thermal-hydraulic models of these reactors are quite different from those of other reactors. The core region of the other conventional reactors is represented by the solid fuel and coolant regions (and maybe moderator region different from coolant region), while MSR contains only liquid fuel. However, the thermal type MSRs may also have graphite zones in the core.

In the literature, several dynamic models are available for circulating fuel reactors (Cammi & Marcello, 2011; El-Sheikh, 2017; Shimazu, 1978; Singh et al., 2018; Zarei, 2019). These models are generally developed for thermal reactors with a graphite moderator. Therefore, a thermal-hydraulic model is also created for the graphite zone in the core. In these studies, the fuel region is generally modeled as two lumped regions. One of the most significant reasons to do this is to be able to write the state equation of the core outlet temperature.

In some studies (El-Sheikh, 2017; Zarei, 2019; Zhang, Qiu & Su, 2009), one or two lumped regions are used for the thermal-hydraulic model. Besides, more than two lumped regions were also used in several studies (Shimazu, 1978; Singh et al., 2018). By increasing the lumped region in the core, the core outlet temperature can be approximated more accurately. In all studies, it is assumed that the core outlet temperature is equal to the average temperature of the upper lumped region.

State-space equations for the thermal-hydraulic modeling of the reactors are generated by using the energy balance for each control volume of the core and heat exchanger (HX) unit. The change in the average temperature of the control volumes can be defined depending on (1) the temperature of the fluid entering that volume, (2) the temperature of the fluid leaving that volume, and (3) the external heat sources.

As above mentioned, when the models available in the literature are examined, for all of them, it is assumed that the outlet temperature of the reactor core is equal to the average temperature of the last of the lumped regions in the core (Cammi & Marcello, 2011; El-Sheikh, 2017; Shimazu, 1978; Singh et al., 2018; Zarei, 2019; Zhang, Qiu & Su, 2009). If the core temperature rise in MSRs is assumed to be around 100 °C, calculation of the core outlet temperature will be quite inaccurate by using this approach in the literature.

In this study, a new approach is proposed to solve this problem. In the core model, energy balance equation for fuel temperature is written without using any assumption and using a single lumped zone. In that condition, one more balance equation has to be taken into account to determine the core outlet temperature. In this study, the required balance equation is formed by using the control volume of the pipeline at the core outlet. Since the temperature difference in the pipe section is very low (compared to the core region) due to the insulation, the core outlet temperature can be calculated more accurately by using this method.

2. Materials and Method

In order to solve the thermal and neutronic characteristics of conceptual Molten Salt Reactors, a simplified model for the primary side is adopted. The schematic view of the conceptual MSR is presented in Figure 1.

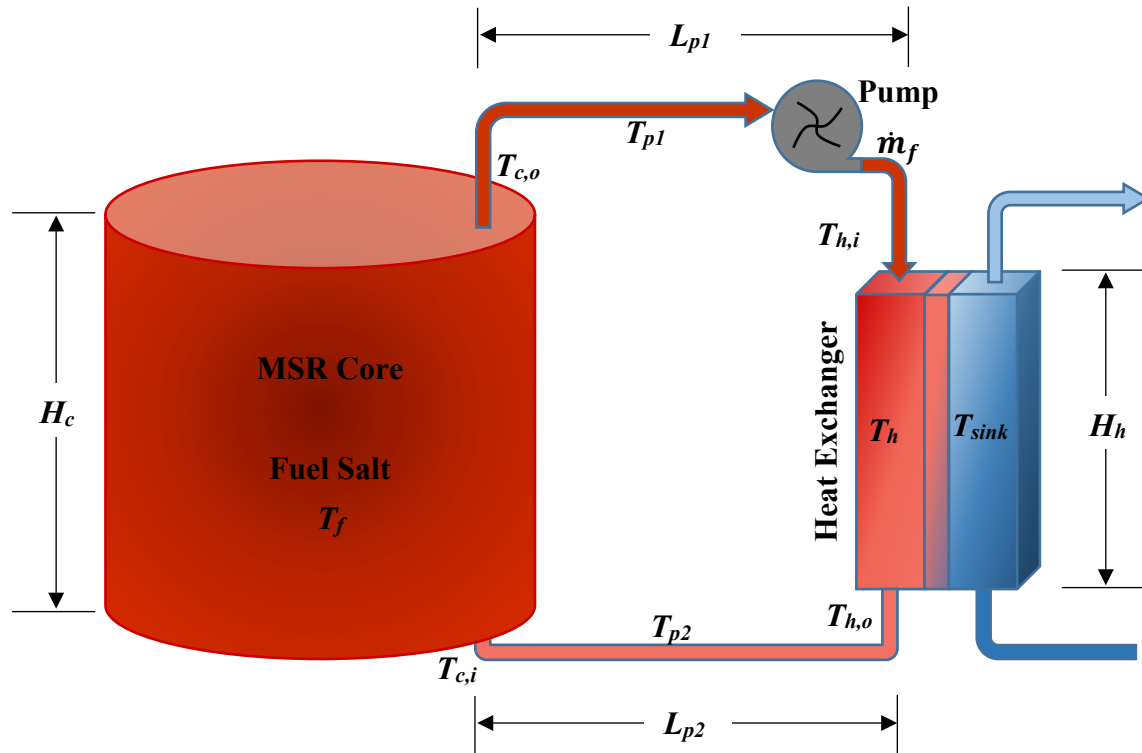


Figure 1: Schematic view of the Molten Salt Reactor primary circuit.

There are several conceptual designs for MSR available in the literature (Antonio Cammi, Marcello, Luzzi, Memoli, & Ricotti, 2011; Serp et al., 2014). It can be thermal or fast, breeder or burner, chloride fueled or fluoride fueled, etc. In this study, a fast spectrum reactor model is adopted. There is no graphite in the system.

Reactor core consists of only liquid fuel, so the thermal model is created for just one-lumped fuel region. There is one circulating pump located upper side of the heat exchanger unit. For the heat exchanger model, the heat transfer mechanism is simulated with the assumption of a "cooler" operating at a constant temperature. The heat transfer between the hot and cold sides is calculated using average temperatures. The heat transfer coefficient is assumed to be constant.

2.1. Mathematical Model

The point kinetic model of MSR core has been represented with one group of delayed neutrons in this study. For the reactivity feedback mechanism, only the variation in fuel temperature has been considered. The lumped method is used for the fuel salt in both reactor core and heat exchanger units.

2.1.1 Reactor neutronics

For the circulating fuel salt, power is generated both inside and outside the core due to the prompt and delayed neutrons. Point kinetic equations derived for these regions are given in Eqs. (1) and (2) (Shimazu, 1978).

$$\frac{dP(t)}{dt} = \frac{\rho_{net}(t) - \beta_{eff}}{\Lambda} P(t) + \lambda_{eff} C(t), \quad (1)$$

$$\frac{dC(t)}{dt} = \frac{\beta_{eff}}{\Lambda} P(t) - \lambda_{eff} C(t) - \frac{1}{\tau_{core}} C(t) + \frac{e^{-\lambda_{eff}\tau_{loop}}}{\tau_{core}} C(t - \tau_{loop}), \quad (2)$$

where P and C represent reactor power and delayed neutron precursor concentration, respectively. The terms ρ_{net} , β_{eff} , λ_{eff} and Λ represent net reactivity, effective delayed neutron fraction, effective delayed neutron decay constant and neutron generation time, respectively. τ represents transit time. Fuel salt passes through the core, pipe section #1, heat exchanger and pipe section #2, respectively and enters the core again (see Figure 1). τ_{loop} represents the transit time out of the core region and it is expressed as, $\tau_{loop} = \tau_{p1} + \tau_{p2} + \tau_h$, where subscripts $p1$, $p2$ and h represent pipe section #1, pipe section #2 and heat exchanger, respectively.

2.1.2 Reactor thermal-hydraulics

The thermodynamic characteristic of the core region is represented by one region fuel lump. The average temperature of the lumped region represents the core fuel temperature. In this study, energy balance is determined via a dimensionless (0-D) model. It is assumed that the specific heat capacity is constant and it is computed at an average temperature of the fuel. The balance equation for the core region can be expressed as

$$m_f c_{p,f} \frac{dT_f(t)}{dt} = P(t) - \dot{m}_f c_{p,f} [T_{c,o}(t) - T_{c,i}(t)], \quad (3)$$

where m_f and \dot{m}_f represent the fuel mass in the core and fuel mass flow rate, respectively. $c_{p,f}$ represents the average heat capacity of the fuel in the core. T_f , $T_{c,i}$ and $T_{c,o}$ represent core lumped fuel temperature, core inlet temperature, and core outlet temperature, respectively.

The balance equation for fuel side of the HX unit can be expressed as

$$m_h c_{p,h} \frac{dT_h(t)}{dt} = \dot{m}_h c_{p,h} [T_{h,i}(t) - T_{h,o}(t)] - (UA)_h [T_h(t) - T_{sink}(t)], \quad (4)$$

where m_h and \dot{m}_h represent the fuel mass in the HX and fuel mass flow rate ($\dot{m}_h = \dot{m}_f$), respectively. $c_{p,h}$ represents the average heat capacity of the fuel in the HX. T_h , $T_{h,i}$, $T_{h,o}$ and T_{sink} represent lumped fuel temperature in the HX, inlet temperature of the HX, outlet

temperature of the HX and average temperature of the heat sink, respectively. U and A_h represent the overall heat transfer coefficient for the HX unit and heat transfer area of the HX, respectively. It is assumed that the overall heat transfer coefficient is constant in this study.

The balance equation for the pipe section #1 can be expressed as

$$m_{p1}c_{p,p1}\frac{dT_{p1}(t)}{dt} = \dot{m}_{p1}c_{p,p1}[T_{c,o}(t) - T_{h,i}(t)] - (UA)_{p1}[T_{p1}(t) - T_{\infty}], \quad (5)$$

where subscript $p1$ represents the pipe section #1. T_{p1} and T_{∞} represent lumped fuel temperature in pipe section #1 and ambient temperature, respectively. It is assumed that the overall heat transfer coefficient is also constant for pipe section #1.

2.1.3 Reactivity feedback mechanism

The net reactivity for the MSR can be expressed as

$$\rho_{net}(t) = \rho_0 + \rho_{ext}(t) - \alpha_f[T_f(t) - T_{f0}], \quad (6)$$

where ρ_0 represents initial balancing reactivity, ρ_{ext} represents external reactivity which can be added with bubbles, α_f represents the core-fuel temperature coefficient of reactivity and T_{f0} represents the steady-state fuel temperature in the core.

2.2. State-Space Representation

The nonlinear differential equations introduced in Section 2.1 may be written in linear form by considering small perturbation around the steady-state operating point. These equations can then be transformed into a state-space model form. Around the steady-state power (P_0 and C_0), Eqs. (1) and (2) can be written as

$$\delta\dot{P}(t) = \frac{P_0}{\Lambda}\delta\rho(t) + \frac{\delta\rho(t)\delta P(t)}{\Lambda} - \frac{\beta_{eff}}{\Lambda}\delta P(t) + \lambda_{eff}\delta C(t), \quad (7)$$

$$\delta\dot{C}(t) = \frac{\beta_{eff}}{\Lambda}\delta P(t) - (\lambda_{eff} + \frac{1}{\tau_{core}})\delta C(t) + \frac{e^{-\lambda_{eff}\tau_{loop}}}{\tau_{core}}\delta C(t - \tau_{loop}), \quad (8)$$

where $P(t) = P_0 + \delta P(t)$, $C(t) = C_0 + \delta C(t)$ and $\rho(t) = \delta\rho(t) = \alpha_f[T_f(t) - T_{f0}]$ due to the nature of the reactivity. The reactor has to be critical at steady-state operation, so the reference reactivity ($\rho_0 + \rho_{ext}$) will be zero at this point.

The nonlinear term, $\delta\rho(t)\delta P(t)$, is still exist in Eq (7). It can be inferred that the point kinetics equations is linear only for constant reactivity conditions. To perform linear analysis, this second-order term is neglected in this study.

Lumped fuel temperatures for the core and the HX regions can be calculated as

$$T_f(t) = \frac{1}{2} [T_{c,o}(t) + T_{c,i}(t)] \quad (9)$$

and

$$T_h(t) = \frac{1}{2} [T_{h,o}(t) + T_{h,i}(t)] \quad (10)$$

respectively. By taking consideration of the transit times at pipe sections #1 and #2, the following substitutions:

$$T_{h,i}(t) \approx T_{c,o}(t - \tau_{p1}) \quad (11)$$

and

$$T_{c,i}(t) \approx T_{h,o}(t - \tau_{p2}) \quad (12)$$

can be made to state the relations between the temperatures. Amount of temperature decrease of fuel salt in the pipeline is neglected due to the insulation. With using Eqs. (9) to (12), Eqs. (3), (4) and (5) can be written in the following forms:

$$m_f c_{p,f} \dot{T}_f(t) = P_0 + \delta P(t) - \dot{m}_f c_{p,f} [T_{c,o}(t) + T_{c,o}(t - \tau_{p1} - \tau_{p2}) - 2T_h(t - \tau_{p2})], \quad (13)$$

$$m_h c_{p,h} \dot{T}_h(t) = 2\dot{m}_h c_{p,h} [T_{c,o}(t - \tau_{p1}) - T_h(t)] - (UA)_h [T_h(t) - T_{sink}] \quad (14)$$

and

$$m_{p1} c_{p,p1} \dot{T}_{c,o}(t) = \dot{m}_{p1} c_{p,p1} [T_{c,o}(t) - T_{c,o}(t - \tau_{p1})] - (UA)_{p1} [T_{c,o}(t) + T_{c,o}(t - \tau_{p1}) - 2T_\infty]/2 \quad (15)$$

where $T_{p1}(t) = 1/2 [T_{c,o}(t) + T_{c,o}(t - \tau_{p1})]$. It is assumed that $\dot{T}_{p1}(t) \approx \dot{T}_{c,o}(t)$ and T_{sink} is constant.

Finally, for the Eqs. (7), (8), (13), (14) and (15) take the state space form as follows:

$$\delta \dot{x} = A_1 x + A_2 x * \delta(t - \tau_{loop}) + A_3 x * \delta(t - \tau_{p1}) + A_4 x * \delta(t - \tau_{p1} - \tau_{p2}) + Bu, \quad (16)$$

where

$$x = [\delta P(t) \quad \delta C(t) \quad T_f(t) \quad T_h(t) \quad T_{c,o}(t)]^T, \quad (17)$$

$$A_1 = \begin{bmatrix} -\frac{\beta_{eff}}{\Lambda} & \lambda_{eff} & \frac{\alpha_f P_0}{\Lambda} & 0 & 0 \\ \frac{\beta_{eff}}{\Lambda} & -\lambda_{eff} - \frac{1}{\tau_{core}} & 0 & 0 & 0 \\ \frac{1}{m_f c_{p,f}} & 0 & 0 & \frac{2\dot{m}_f}{m_f} & -\frac{\dot{m}_f}{m_f} \\ 0 & 0 & 0 & -\frac{2\dot{m}_f}{m_f} - \frac{(UA)_h}{m_f c_{p,h}} & 0 \\ 0 & 0 & 0 & 0 & \frac{\dot{m}_f}{m_f} - \frac{(UA)_{p1}}{2m_f c_{p,p1}} \end{bmatrix}, \quad (18)$$

$$A_2 = \begin{bmatrix} 0 & 0 & 0 & 0 & 0 \\ 0 & e^{-\lambda_{eff} \tau_{loop} / \tau_{core}} & 0 & 0 & 0 \\ 0 & 0 & 0 & 0 & 0 \\ 0 & 0 & 0 & 0 & 0 \\ 0 & 0 & 0 & 0 & 0 \end{bmatrix}, \quad (19)$$

$$A_3 = \begin{bmatrix} 0 & 0 & 0 & 0 & 0 \\ 0 & 0 & 0 & 0 & 0 \\ 0 & 0 & 0 & 0 & 0 \\ 0 & 0 & 0 & 0 & \frac{2\dot{m}_f}{m_f} \\ 0 & 0 & 0 & 0 & -\frac{\dot{m}_f}{m_f} - \frac{(UA)_{p1}}{2m_f c_{p,p1}} \end{bmatrix}, \quad (20)$$

$$A_4 = \begin{bmatrix} 0 & 0 & 0 & 0 & 0 \\ 0 & 0 & 0 & 0 & 0 \\ 0 & 0 & 0 & 0 & -\frac{\dot{m}_f}{m_f} \\ 0 & 0 & 0 & 0 & 0 \\ 0 & 0 & 0 & 0 & 0 \end{bmatrix}, \quad (21)$$

$$B = \begin{bmatrix} -\frac{\alpha_f P_0}{\Lambda} & 0 & 0 & 0 & 0 \\ 0 & 0 & \frac{1}{m_f c_{p,f}} & 0 & 0 \\ 0 & 0 & 0 & \frac{(UA)_h}{m_f c_{p,h}} & 0 \\ 0 & 0 & 0 & 0 & \frac{(UA)_{p1}}{m_f c_{p,p1}} \end{bmatrix}^T \quad (22)$$

and

$$u = [T_{f0} \quad P_0 \quad T_{sink} \quad T_{\infty}]^T. \quad (23)$$

It is important to note that $\dot{m}_f = \dot{m}_h = \dot{m}_{p1} = \dot{m}_{p2}$ due to the closed-loop operation (variation of expansion tank level is neglected). All physical properties are taken as constant and calculated at the average temperature of lumped regions. Transit time can be calculated by dividing system length (or height) by velocity of the fluid.

3. MATLAB-Simulink Model

The primary loop of MSR is simulated under steady-state condition using MATLAB Simulink (*MATLAB-Simulink User's Guide R2019b*, 2019). The dynamic model configuration is presented in Figure 2. Core dynamic model consists of neutronic and thermal-hydraulic coupled system. Coupling is provided with the reactivity feedback mechanism. Therefore, by doing so a tool to make analysis with the new modeling has been generated.

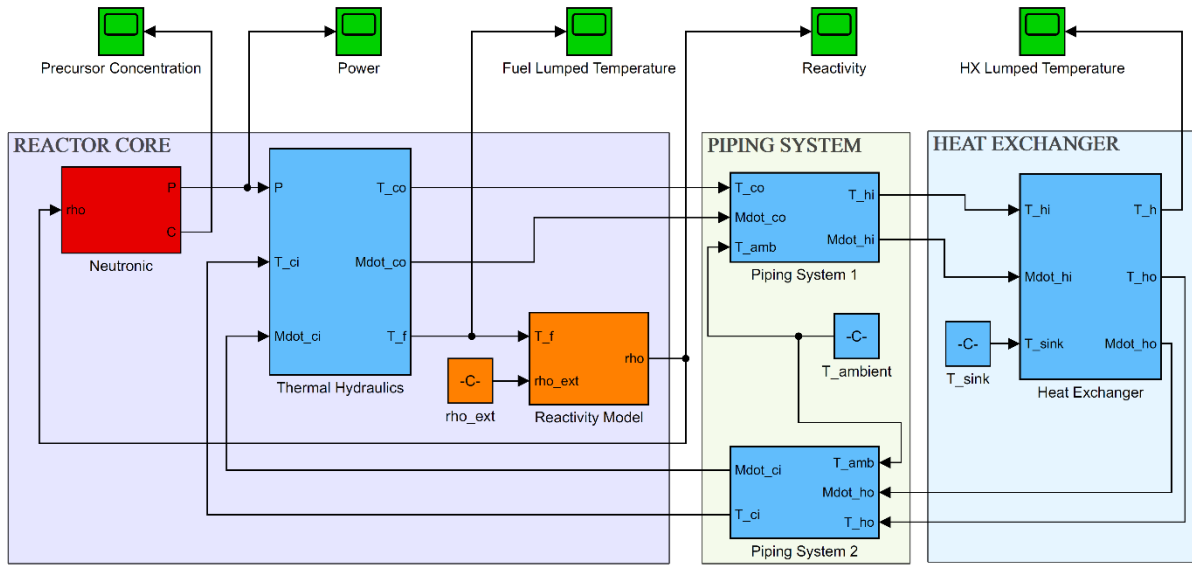


Figure 2: Simulink model

In this tool, the input parameters are external reactivity, ambient temperature and heat sink temperature. The output values are mainly reactor power and the core outlet temperature.

There are several different MSR concepts presented in the literature. Therefore, there is a wide variety of values for both input and output parameters. Table 1 presents the MSR (fast or thermal) parameters and their value ranges that can be used for the developed model and the tool. The proposed model and derived state-space equations can be used for any specific fast MSRs. The equations are written for generic parameters.

Table 1: MSR parameters and the range of values

Parameters	Sym.	Unit	Range in literature ^(*)
Reactor power	P	MWth	300 – 3000
Prompt neutron generation time	Λ	s	$10^{-7} - 10^{-6}$
Initial balancing reactivity	ρ_0	pcm	$\beta_{eff} \left[\frac{1 - e^{-\lambda_{eff}\tau_{loop}}}{\lambda_{eff}\tau_{core} + 1 - e^{-\lambda_{eff}\tau_{loop}}} \right]$
Steady state external reactivity	ρ_{ext}	pcm	$\rho_{ext} = -\rho_0$
Effective delayed neutron fraction	β_{eff}	-	~ 0.0033

Effective delayed neutron decay constant	λ_{eff}	s^{-1}	~ 0.06
Core transit time	τ_{core}	s	$\sim m_f / \dot{m}_f$
Loop transit time	τ_{loop}	s	$\tau_h + \tau_{p1} + \tau_{p2}$
Pipe section #1 transit time	τ_{p1}	s	$\sim m_{p1} / \dot{m}_f$
Pipe section #2 transit time	τ_{p2}	s	$\sim m_{p2} / \dot{m}_f$
Heat exchanger transit time	τ_h	s	$\sim m_h / \dot{m}_f$
Fuel temperature coefficient of reactivity	α_f	K^{-1}	$\sim 3.4 \times 10^{-5}$
Fuel mass flow rate	\dot{m}_f	$kg \cdot s^{-1}$	depends on the power
Fuel mass in the core	m_f	kg	$d_f @ T_f V_{core}$
Fuel mass in the HX	m_h	kg	$d_f @ T_h V_h$
Fuel mass in the pipe section #1	m_{p1}	kg	$d_f @ T_{p1} V_{p1}$
Fuel mass in the pipe section #2	m_{p2}	kg	$d_f @ T_{p2} V_{p2}$
Specific heat capacity of the fuel	c_p	$J \cdot kg^{-1} K^{-1}$	$-1111 + 2.782 T_f$
Heat exchanger heat transfer coefficient	$(UA)_h$	$W \cdot K^{-1}$	$P = N_{HX} (UA)_h \Delta T_{lm}^{(**)}$
Average fuel temperature (in the core)	T_f	K	~ 975
Average fuel temperature (in the HX)	T_h	K	~ 975
Average temperature of the heat sink	T_{sink}	K	750-900
Ambient temperature	T_{∞}	K	~ 300
Density of the fuel salt	d_f	$kg \cdot m^{-3}$	$4983.56 - 0.882 T_f$
Volume of the core	V_{core}	m^3	depends on the power
Volume of the HX	V_h	m^3	depends on the HX capacity
Volume of the pipelines #1, #2	$V_{p1,p2}$	m^3	depends on the design

(*) (Aufiero et al., 2014; Fiorina et al., 2014; Köse, Koç, Erbay, Ögüt, & Ayhan, 2019; Lecce, 2018; Merle-Lucotte et al., 2012)

(**) N_{HX} represents number of HX unit in the design and ΔT_{lm} is the log mean temperature difference.

4. Results

In this study general Simulink model was developed for fast type MSR. There is only liquid fuel in the core. Unlike the thermal MSR, there is no graphite moderator in the core region. The values in the Table 1 are reactor dependent parameters. There is no available fast type MSR in operation right now. However, there are several publications for the fast type concept MSR. Reactor parameters used in the simulations are presented in Table 2.

Table 2: Fast type MSR parameters used in the simulation

Parameters	Value
Reactor power	3000 MWth
Average core temperature	700 °C
Core transit time	2 s
Loop transit time	2 s
Transit time for each pipes	0.1 s
Effective delayed neutron fraction	0.0033
Effective delayed neutron decay constant	$0.0611 s^{-1}$
Prompt neutron generation time	$0.95e-6 s$
Fuel temperature coefficient of reactivity	$3.4e-5 K^{-1}$
Coolant bulk temperature	570 °C
Ambient temperature	40 °C

For the steady state operation, power profile, precursor concentration and fuel temperature of the core and heat exchanger regions are presented in Figure 3.

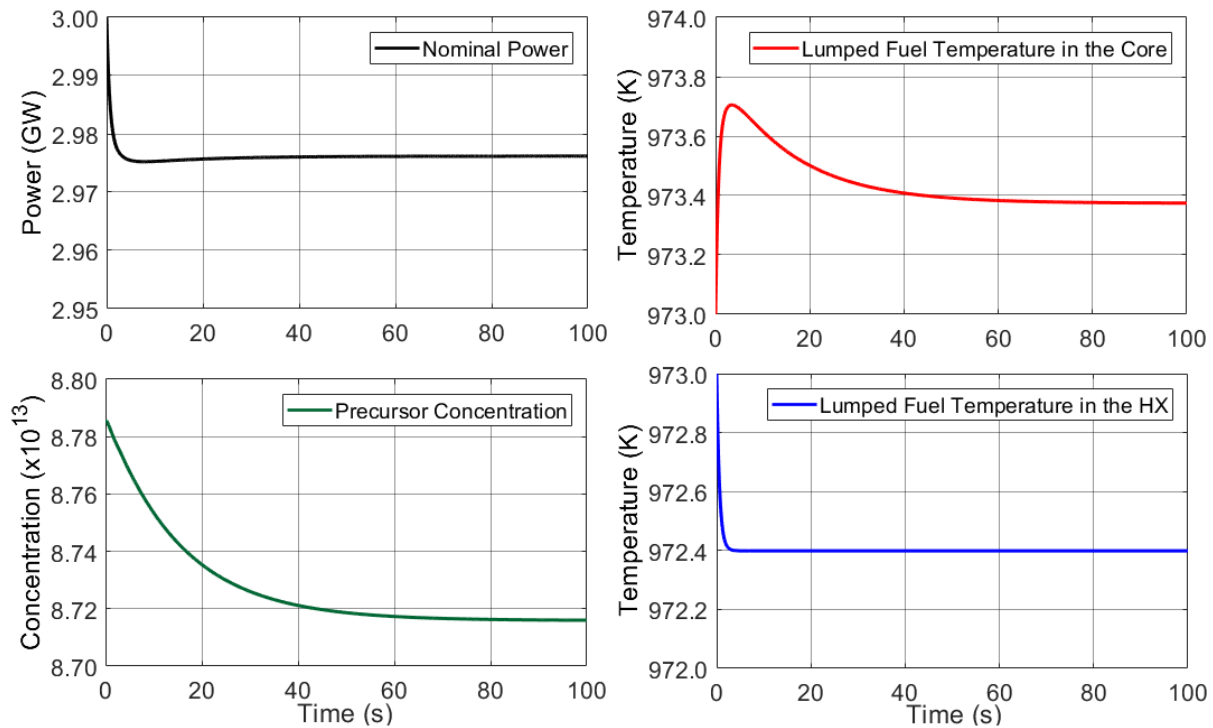


Figure 3: Reactor parameters at steady state operation

As seen in Figure 3, the reactor reaches thermal equilibrium at 2.98 GW with the parameters in Table 2. After about 100 s, the reactor reaches steady-state operation level. Temperature differences between the fuel temperatures of the core region and the HX region are so small. There is about 1 K temperature decrease due to the heat loss at pipelines. In this concept reactor, there is 100 K increase in fuel temperature across the core.

The fast type MSRs can be simulated with the proposed model. This model can also be used for perturbation cases. Parameters for the reactor system of fast MSR is adopted from literature (Köse et al., 2019; Lecce, 2018; Merle-Lucotte et al., 2012). The results are consistent with each other and the values are meaningful compared with these studies.

5. Conclusion

There are several dynamic models for thermal Molten Salt Reactors in the literature. In these studies, two or more lumped regions have been used at the reactor core for thermal-hydraulic modeling. Furthermore, in all of them, it is assumed that the core outlet temperature is equal to the average temperature of the upper lumped region. However, by this assumption, calculated core outlet temperature will be inaccurate due to the significant temperature rise in the reactor core.

For all types of MSR, one of the main concern is circulating fuel. For thermal or fast spectrum types, there are no significant differences in terms of the core dynamic model for the fuel side. On the other hand, there is a significant difference in the thermal reactor model due

to the moderator region. Graphite region has to be modeled due to the feedback effect of moderator temperature in the thermal MSR. There is no moderator region in the fast MSR.

In this study, a new dynamic model is proposed for the fast MSR. One lumped region has been adopted for reactor core since there is only fuel salt in the core. The energy balance for the core outlet temperature has been determined using pipeline temperature. The nonlinear point kinetic equation has been linearized about the point of steady-state operation condition. State-space form was obtained and MATLAB-Simulink model was created using this form. The proposed model was tested for conceptual reactor using available data from the literature. The proposed final model can be used for all kinds of fast MSR since generic parameters for the fast type MSR are used in this model.

6. References

- 1) Aufiero, M., Cammi, A., Geoffroy, O., Losa, M., Luzzi, L., Ricotti, M. E., & Rouch, H. (2014). Development of an OpenFOAM model for the Molten Salt Fast Reactor transient analysis. *Chemical Engineering Science*, 111, 390–401. <https://doi.org/10.1016/j.ces.2014.03.003>
- 2) Cammi, A., & Marcello, V. Di. (2011). Transfer Function Modeling of Zero-Power Dynamics of Circulating Fuel Reactors. *Journal of Engineering for Gas Turbines and Power*, 133, 1–8. <https://doi.org/10.1115/1.4002880>
- 3) Cammi, Antonio, Marcello, V. Di, Luzzi, L., Memoli, V., & Ricotti, M. E. (2011). A multi-physics modelling approach to the dynamics of Molten Salt Reactors. *Annals of Nuclear Energy*, 38(6), 1356–1372. <https://doi.org/10.1016/j.anucene.2011.01.037>
- 4) El-Sheikh, B. M. (2017). Kinetic Analysis of Molten Salt Reactors. *Arab Journal of Nuclear Sciences and Applications*, 50(4), 201–212.
- 5) Fiorina, C., Lathouwers, D., Aufiero, M., Cammi, A., Guerrieri, C., Leen, J. & Enrico, M. (2014). Modelling and analysis of the MSFR transient behaviour. *Annals of Nuclear Energy*, 64, 485–498. <https://doi.org/10.1016/j.anucene.2013.08.003>
- 6) Köse, U., Koç, U., Erbay, L. B., Öğüt, E. & Ayhan, H. (2019). Heat exchanger design studies for Molten Salt Fast Reactor. *EPJ Nuclear Science & Technology*. <https://doi.org/https://doi.org/10.1051/epjn/2019032>
- 7) Lecce, F. Di. (2018). Neutronic and thermal-hydraulic simulations for Molten Salt Fast Reactor safety assessment. *Politecnico Di Torino*.
- 8) MATLAB-Simulink User's Guide R2019b. (2019). The MathWorks Inc. Retrieved from https://www.mathworks.com/help/pdf_doc/simulink/sl_using.pdf
- 9) Merle-Lucotte, E., Heuer, D., Allibert, M., Brovchenko, M., Ghetta, V., Laureau, A., & Rubiolo, P. (2012). Preliminary Design Assessment of the Molten Salt Fast Reactor. In *ECN-2012: Transactions Advanced Reactors* (pp. 17–26).
- 10) Serp, J., Allibert, M., Ghetta, V., Heuer, D., Holcomb, D., Ignatiev, V. & Zhimin, D. (2014). The molten salt reactor (MSR) in Generation IV: Overview and perspectives. *Progress in Nuclear Energy*, 77, 308–319. <https://doi.org/10.1016/j.pnucene.2014.02.014>

11) Shimazu, Y. (1978). Nuclear Safety Analysis of a Molten Salt Breeder Reactor. *Journal of Nuclear Science and Technology*, 522(July), 514–522.

12) Singh, V., Lish, M. R., Wheeler, A. M., Chvála, O., Singh, V., Lish, M. R. & Upadhyaya, B. R. (2018). Dynamic Modeling and Performance Analysis of a Two-Fluid Molten Salt Breeder Reactor System. *Nuclear Technology*, 1–24.
<https://doi.org/10.1080/00295450.2017.1416879>

13) Zarei, M. (2019). A refined time-delay modeling of the molten salt reactor dynamics. *Progress in Nuclear Energy*, 117, 103102.
<https://doi.org/10.1016/j.pnucene.2019.103102>

14) Zhang, D., Qiu, S. & Su, G. (2009). Development of a safety analysis code for molten salt reactors. *Nuclear Engineering and Design*, 239, 2778–2785.
<https://doi.org/10.1016/j.nucengdes.2009.08.020>